Derna University Journal of Applied Sciences

Vol. 3, Issue 1, 2026

ISSN: 3079-0719 (Online) | DOI: https://doi.org/10.58987/zqzzpe91

Numerical Solution of the SEITR Model with Standard Incidence for Hepatitis B Transmission Using the Fourth-Order Runge–Kutta Method

N. R. F. Elfakhakhre

Department of Mathematics, Faculty of Science, University of Derna, Libya
n.rajab@uod.edu.ly

Received: Jun 05, 2026; **Accepted**: June 27, 2026

Abstract—This study presents a numerical solution to a Susceptible–Exposed–Infected–Treated–Recovered (SEITR) epidemiological model with standard incidence ($\beta SI/N$) for hepatitis B virus (HBV) transmission dynamics. The model is parameterized using real demographic and epidemiological data from Ambon, Indonesia (2020). The resulting system of five nonlinear ordinary differential equations is solved using the classical fourth order Runge Kutta (RK4) method with a time step of $h = 0.01$ years. The numerical implementation is validated through three independent verification tests: *(i)* an empirical order of convergence test confirming that the global error decreases at the theoretically expected fourth order rate as the step size is refined; *(ii)* cross validation against MATLAB's adaptive Runge Kutta Fehlberg solver (ode45), which reproduces the RK4 trajectories for all five subpopulations with absolute differences within 10^{-14}–10^{-8}; and *(iii)* a sensitivity analysis across a range of transmission rates β, showing that the infected subpopulation increases with transmission intensity, consistent with the expected epidemiological behavior of the model. The results confirm that RK4 provides an accurate and numerically stable solution for standard incidence SEITR models and supports its use for evaluating hepatitis B control strategies.

Keywords—Hepatitis B transmission; SEITR model; Standard incidence rate; Fourth order Runge-Kutta method

1. Introduction

Hepatitis B is one of the most dangerous infectious diseases that affect the liver, since its chronic form may develop into cirrhosis or liver cancer. The virus is transmitted mainly through contaminated blood and bodily fluids, unsafe injections, and from mother to fetus. Despite the availability of a safe and effective vaccine for decades, this disease still represents a major global health burden, highlighting the ongoing need for precise quantitative tools to understand the dynamics of its spread and to evaluate the effectiveness of strategies to combat its transmission**.**

Modern epidemiological models are based on dividing the population into homogeneous subpopulations and formulating the infection transmission between them as ordinary differential equations. This approach was applied early to hepatitis B by McLean and Blumberg [1], and then Liang et al. [2] reviewed the development of these models between 1994 and 2015, showing the prevalence of five and six subpopulations. An example of this pattern is the five subpopulations

MSLIR model, which clearly distinguishes between immunized, susceptible, latent, infected, and recovered individuals [3]; while Xue et al. [4] proposed deterministic and stochastic models with a general incidence function.

One of the most important methodological aspects in constructing these models is the choice of the force of infection form, which describes the rate of disease transmission from Infected individuals to susceptible individuals. While the traditional form mass action rate (βSI) assumes that the contact rate between individuals is directly proportional to the absolute population density. This assumption loses its biological realism when applied to large or temporally varying human populations, since the number of actual contacts per individual does not increase without bound as the population size grows. In contrast, the standard incidence form ($\beta SI/N$) normalizes the infection transmission term by the total population size N, so that the individual contact rate remains bounded and independent of the overall size of the community. This makes it a representation more consistent with epidemic behavior and explains its widespread adoption as the most accepted form in modern epidemiological literature [5].

Considering the nature of the infectiousness, Vargas-De-Leon [6] provided a fundamental theoretical treatment of the standard infection rate, demonstrating the global stability of disease-free and endemic equilibrium points in the SIS, SIR, and SIRS models using Lyapunov functions. Based on the (βSI) formula and specifically the SEITR model, Otunuga and Ogunsulu [7] developed a multistage random model. Larobon et al. [8] presented a mathematical analysis of the hepatitis B epidemic spread model in Ambon City, deducing the equilibrium points and the basic reproduction number.

Regardless of the incidence rate formulation adopted, the resulting systems of nonlinear differential equations generally admit no closed form analytical solution, necessitating recourse to numerical techniques. Among these, the fourth–order Runge Kutta method (RK4) has been extensively employed in the numerical solution of epidemic models. Papalia et al. [9] applied RK4 to an SEIR model of hepatitis B transmission in the city of Ambon; notably, neither of the previous studies incorporated a distinct treatment compartment within the model structure. Other authors have compared RK4 against the Euler method across various epidemic models, demonstrating its superior accuracy and numerical stability relative to lower order methods [10,11], while Khoiri et al. [12] examined the numerical stability bounds and positivity conditions of RK4 as applied to a vaccination-extended SEIR model. More recently, research attention has shifted toward fractional-order formulations capable of capturing memory and hereditary effects in disease progression [13,14]. In this context, Mtawal et al. [15] proposed a novel hybrid analytical technique (MSYTVHPM) to efficiently solve the fractional order SIR epidemic model. However, such approaches introduce additional mathematical complexity associated with the selection of the fractional order kernel and the biological interpretation of the fractional parameter, which may complicate both analytical tractability and clinical applicability.

This study formulates a SEITR model for hepatitis B transmission using a standard incidence formulation and solves the resulting system with the fourth–order Runge Kutta method. Using demographic and epidemiological data representative of Ambon, Indonesia, the model's behavior is examined across a range of values of the transmission coefficient β. Three verification steps were carried out: a convergence test for the RK4 method, a comparison with MATLAB's ode45 solver,

and a sensitivity analysis examining how each subpopulation (S, E, I, T, and R) responds to changes in transmission intensity.

2. Mathematical Model

The SEITR model of Hepatitis B disease spread in this study divides the total population into five subpopulation variables with the following assumptions:

- Natural mortality occurs in all subpopulations, at the constant rate μ_1 while infected individuals are additionally subject to a disease induced mortality rate μ_2.
- The Susceptible subpopulation $S(t)$ comprises individuals at risk of infection but not yet infected. It increases by the birth of unvaccinated individuals entering at a rate of $(1-\sigma)\kappa N$ and is depleted by infection and natural mortality.
- The Exposed subpopulation $E(t)$comprises individuals who carry the virus during the incubation period but are not yet symptomatic or infectious. It increases through contact between Susceptible and Infectious individuals, governed by the standard incidence rate $\beta SI/N$, the transmission term is normalized by the total population $N(t)$, so that the per-capita contact rate remains bounded and independent of population size.
- The Infected subpopulation $I(t)$ comprises individuals who are actually infected and capable of transmitting the infection; individuals progress from E to I at rate α.
- The Treatment subpopulation $T(t)$ comprises infected individuals who have begun receiving medical care and treatment; individuals move from I to T at rate γ.
- The Recovered subpopulation $R(t)$ comprises individuals who have recovered following treatment, entering from T at rate δ, together with vaccinated newborns, who enter R directly at rate $\sigma\kappa N$.
- The total population $N(t) = S(t) + E(t) + I(t) + T(t) + R(t)$ is not constant. It varies over time as a result of births and of both natural and disease induced deaths. The standard incidence formulation $\beta SI/N$ is adopted specifically to preserve physical consistency and prevent unrealistic numerical growth as $N(t)$ evolves a consideration that does not arise under the mass action form βSI, where N is implicitly assumed constant.
- Recovered individuals do not revert to the Susceptible class, as they are assumed to acquire durable immunity, whether through natural recovery after treatment or through vaccination at birth.

The total population $N(t)$ at any given time t is $N(t) = S(t) + E(t) + I(t) + T(t) + R(t)$). As shown in the flow diagram in Figure 1, unvaccinated individuals enter the subpopulation S at a rate $(1-\sigma)\kappa N$, while vaccinated individuals enter directly into the subpopulation R at a rate of $\sigma\kappa N$; individuals move from S to E with a $\beta SI/N$ infection strength, from E to I at a rate of α, from I to T at a rate of γ, and from T to R at a rate of δ; each subpopulation leaves at a normal mortality rate of μ_1, with an additional mortality rate of μ_2 from the infected class only due to the disease. Based on the flow diagram and adopting the standard incidence formulation described, the following system of nonlinear ordinary differential equations was formulated:

$$\frac{dS}{dt} = (1-\sigma)\kappa N - \beta SI/N - \mu_1 S \quad (1)$$

$$\frac{dE}{dt} = \beta SI/N - (\alpha + \mu_1)E \quad (2)$$

$$\frac{dI}{dt} = \alpha E - (\gamma + \mu_1 + \mu_2)I \quad (3)$$

$$\frac{dT}{dt} = \gamma I - (\mu_1 + \delta)T \quad (4)$$

$$\frac{dR}{dt} = \sigma\kappa N + \delta T - \mu_1 R \quad (5)$$

Where:

κ is the natural birth rate
σ is the vaccination coverage rate.
β is the transmission rate.
α is the rate of progression from exposure to infection.
γ is the percentage of those receiving treatment
δ is the recovery rate after treatment.
$\mu_1$is the natural mortality rate
μ_2 is the mortality rate due to the disease.

The terms $(1-\sigma)\kappa N$ and $\sigma\kappa N$ distribute newborns between the Susceptible and Recovered classes according to the vaccination coverage ratio σ. The remaining terms represent: natural mortality in each subpopulation $(\mu_1 S, \mu_1 E, \mu_1 I, \mu_1 T, \mu_1 R)$; disease induced mortality $(\mu_2 I)$; progression from exposure to infection (αE); entry into Treatment (γI); and Recovery after Treatment (δT).

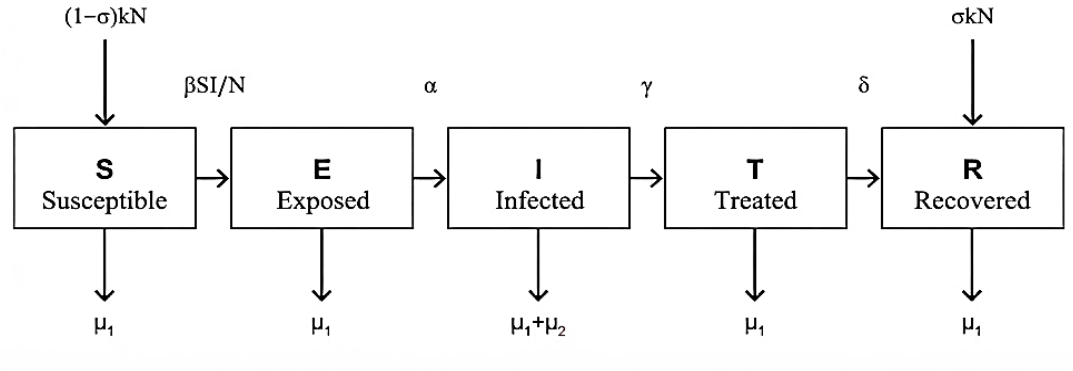

Figure 1. SEITR model flowchart for hepatitis B disease Transmission.

3. Fourth-Order Runge-Kutta Method

The fourth order Runge Kota (RK4) method was used to obtain a high precision approximate numerical solution, given its local accuracy of order $O(h^5)$ for each time step (h) and its good numerical stability when dealing with nonlinear differential systems. Defining the state vector Y and the vector function $f(t, Y)$ representing the right-hand side of to the equations (1-5) as follow:

$$Y = \begin{bmatrix} y_1 \\ y_2 \\ y_3 \\ y_4 \\ y_5 \end{bmatrix} = \begin{bmatrix} S \\ E \\ I \\ T \\ R \end{bmatrix}; \quad f(t,Y) = \begin{bmatrix} (1-\sigma)\kappa N - \beta SI/N - \mu_1 S \\ \beta SI/N - (\alpha + \mu_1)E \\ \alpha E - (\gamma + \mu_1 + \mu_2)I \\ \gamma I - (\mu_1 + \delta)T \\ \sigma\kappa N + \delta T - \mu_1 R \end{bmatrix}$$

Four approximate slopes are calculated for each time step from time t_n to time $t_{n+1} = t_n + h$ according to the following formulas:

$$k_1 = f(t_n, Y_n) \tag{6}$$

$$k_2 = f(t_n + \frac{h}{2}, Y_n + \frac{h}{2} k_1) \tag{7}$$

$$k_3 = f\left(t_n + \frac{h}{2}, Y_n + \frac{h}{2} k_2\right) \tag{8}$$

$$k_4 = f(t_n + h, Y_n + hk_3) \tag{9}$$

The state vector for the next time step is then updated with the weighted average of the four trends:

$$Y_{n+1} = Y_n + \frac{h}{6}(k_1 + 2k_2 + 2k_3 + k_4) \tag{10}$$

The system of equations consisting of Equations (1-5) is substituted in to the RK4 to obtain Equations

$$S_{n+1} = S_n + \frac{h}{6}(k_{1s} + 2k_{2s} + 2k_{3s} + k_{4s}) \tag{11}$$

$$E_{n+1} = E_n + \frac{h}{6}(k_{1E} + 2k_{2E} + 2k_{3E} + k_{4E}) \tag{12}$$

$$I_{n+1} = I_n + \frac{h}{6}(k_{1I} + 2k_{2I} + 2k_{3I} + k_{4I}) \tag{13}$$

$$T_{n+1} = T_n + \frac{h}{6}(k_{1T} + 2k_{2T} + 2k_{3T} + k_{4T}) \tag{14}$$

$$R_{n+1} = R_n + \frac{h}{6}(k_{1R} + 2k_{2R} + 2k_{3R} + k_{4R}) \tag{15}$$

Where:

$$N_n = S_n + E_n + I_n + T_n + R_n$$

$$k_{1s} = f_s(t_n, Y_n) = (1-\sigma)\kappa N_n - \beta S_n I_n / N_n - \mu_1 S_n$$

$$k_{1E} = f_E(t_n, Y_n) = \beta S_n I_n / N_n - (\alpha + \mu_1) E_n$$

$$k_{1I} = f_I(t_n, Y_n) = \alpha E_n - (\gamma + \mu_1 + \mu_2) I_n$$

$$k_{1T} = f_T(t_n, Y_n) = \gamma I_n - (\mu_1 + \delta) T_n$$

$$k_{1R} = f_R(t_n, Y_n) = \sigma\kappa N_n + \delta T_n - \mu_1 R_n$$

$$N^{(1)}_{n+\frac{h}{2}} = \left(S_n + \frac{h}{2} k_{1s}\right) + \left(E_n + \frac{h}{2} k_{1E}\right) + \left(I_n + \frac{h}{2} k_{1I}\right) + \left(T_n + \frac{h}{2} k_{1T}\right) + \left(R_n + \frac{h}{2} k_{1R}\right)$$

$$k_{2s} = (1-\sigma)\kappa N^{(1)}_{n+\frac{h}{2}} - \frac{\beta(S_n + \frac{h}{2} k_{1s})(I_n + \frac{h}{2} k_{1I})}{N^{(1)}_{n+\frac{h}{2}}} - \mu_1(S_n + \frac{h}{2} k_{1s})$$

$$k_{2E} = \frac{\beta(S_n + \frac{h}{2} k_{1s})(I_n + \frac{h}{2} k_{1I})}{N^{(1)}_{n+\frac{h}{2}}} - (\alpha + \mu_1)(E_n + \frac{h}{2} k_{1E})$$

$$k_{2I} = \alpha(E_n + \frac{h}{2} k_{1E}) - (\gamma + \mu_1 + \mu_2)(I_n + \frac{h}{2} k_{1I})$$

$$k_{2T} = \gamma(I_n + \frac{h}{2} k_{1I}) - (\mu_1 + \delta)(T_n + \frac{h}{2} k_{1T})$$

$$k_{2R} = \sigma\kappa N^{(1)}_{n+\frac{h}{2}} + \delta(T_n + \frac{h}{2}\, k_{1T}) - \mu_1(R_n + \frac{h}{2}\, k_{1R})$$

$$N^{(2)}_{n+\frac{h}{2}} = \left(S_n + \frac{h}{2}\, k_{2s}\right) + \left(E_n + \frac{h}{2}\, k_{2E}\right) + \left(I_n + \frac{h}{2}\, k_{2I}\right) + \left(T_n + \frac{h}{2}\, k_{2T}\right) + (R_n + \frac{h}{2}\, k_{2R})$$

$$k_{3s} = (1-\sigma)\kappa N^{(2)}_{n+\frac{h}{2}} - \frac{\beta(S_n+\frac{h}{2}k_{2s})(I_n+\frac{h}{2}k_{2I})}{N^{(2)}_{n+\frac{h}{2}}} - \mu_1(S_n + \frac{h}{2}\, k_{2s})$$

$$k_{3E} = \frac{\beta(S_n+\frac{h}{2}k_{2s})(I_n+\frac{h}{2}k_{2I})}{N^{(2)}_{n+\frac{h}{2}}} - (\alpha+\mu_1)(E_n + \frac{h}{2}\, k_{2E})$$

$$k_{3I} = \alpha(E_n + \frac{h}{2}\, k_{2E}) - (\gamma + \mu_1 + \mu_2)(I_n + \frac{h}{2}\, k_{2I})$$

$$k_{3T} = \gamma(I_n + \frac{h}{2}\, k_{2I}) - (\mu_1 + \delta)(T_n + \frac{h}{2}\, k_{2T})$$

$$k_{3R} = \sigma\kappa N^{(2)}_{n+\frac{h}{2}} + \delta(T_n + \frac{h}{2}\, k_{2T}) - \mu_1(R_n + \frac{h}{2}\, k_{2R})$$

$$N^{(3)}_{n+h} = (S_n + h\, k_{3s}) + (E_n + h\, k_{3E}) + (I_n + h\, k_{3I}) + (T_n + h\, k_{3T}) + (R_n + h\, k_{3R})$$

$$k_{4s} = (1-\sigma)\kappa N^{(3)}_{n+h} - \frac{\beta(S_n+h\, k_{3s})(I_n+h\, k_{3I})}{N^{(3)}_{n+h}} - \mu_1(S_n + h\, k_{3s})$$

$$k_{4E} = \frac{\beta(S_n+h\, k_{3s})(I_n+h\, k_{3I})}{N^{(3)}_{n+h}} - (\alpha+\mu_1)(E_n + h\, k_{3E})$$

$$k_{4I} = \alpha(E_n + h\, k_{3E}) - (\gamma + \mu_1 + \mu_2)(I_n + h\, k_{3I})$$

$$k_{4T} = \gamma(I_n + h\, k_{3I}) - (\mu_1 + \delta)(T_n + h\, k_{3T})$$

$$k_{4R} = \sigma\kappa N^{(3)}_{n+h} + \delta(T_n + h\, k_{3T}) - \mu_1(R_n + h\, k_{3R})$$

4. Algorithm

Algorithm: SEITR Model Simulation

- Initialize Parameters: Set $\gamma, \beta, \delta, \alpha, \sigma, \mu_1,\ \mu_2$ and κ.
- Set Initial State: Define vector $Y_0 = [S_0, E_0, I_0, T_0, R_0]$.
- Define Time Step: Set total years T and time step $h = 0.01$.
- Loop for each time step t from 0 to T/h:
  - Calculate $N_t = \sum(Y_t)$.
  - Update System Equations (1-5).
  - Apply RK4.
- Output Results: Store values for each year and export to table

5. Numerical Model Simulation

To validate the proposed model, it was empirically applied to demographic and epidemiological data pertaining to the city of Ambon, Indonesia, for the year 2020 [8]. The relevant parameters were estimated based on real data obtained from the local health authority. Table (1) shows the initial conditions adopted at time t = 0, while Table (2) presents the numerical values of the model's fixed parameters.

Table 1. Initial values for subpopulations on $t = 0$, [8].

$\mathbf{S(0)}$	$\mathbf{E(0)}$	$\mathbf{I(0)}$	$\mathbf{T(0)}$	$\mathbf{R(0)}$
121663	0	792	124	225646

Table 2. Parameter values**,** [8].

Parameters	**Definition**	**value**
κ	Natural birth rate	0,0153
σ	Rate of vaccinated individuals	0.6497
α	Rate of exposed individuals becoming infected	4
γ	Rate of infected individuals on treatment	0.1354
δ	Rate of individuals who recover after treatment	1
μ_1	Natural mortality rate	0.0141
μ_2	Death rate due to Hepatitis B infection	0

Given the rapid transition dynamics from the Exposed to the Infected area ($\alpha = 4$), a relatively small step of $h = 0.01$ years was adopted throughout the calculation to ensure the numerical stability of the solution. A value of $h = 0.01$ effectively mitigates numerical oscillations, prevent truncation errors associated with explicit Runge Kutta formulas, and ensure stable convergence across all simulated subpopulations. To realistically represent the populations, the calculated values were recorded and rounded to the nearest whole number at the end of each full year. The simulation starting from the initial conditions listed in Table 2, using MATLAB software implementing the algorithm.

Table 3 presents the simulation results every five years over 100 years under $\beta = 0.45$. The Susceptible subpopulation S increases steadily from 121663 to 130024, consistent with a continuous inflow of unvaccinated newborns. The Exposed subpopulation E rises quickly to around 33 individuals within the first 20 years, then stabilizes at 35 by year 40. The Infected subpopulation I decreases initially from 792, then rises gradually to a maximum of 945 around year 75, before declining slightly to 932 by year 100. The Treatment subpopulation T follows a similar pattern, dropping from 124 to a minimum of 105 around year 5, then increasing to a plateau of 125-126 from about year 60 onward. The Recovered subpopulation R increases steadily throughout, from 225646 to 261507. Overall, the Infected and Treated subpopulations remain at a substantial, persistent level rather than declining toward zero.

Four different β values were simulated over 100 years to analysis sensitivity of transition rate (β) as shown in Figures (2–6). For the lower values ($\beta = 0.07, 0.30$), Susceptible individuals decline briefly before recovering, while Exposed, Infected, and Treatment subpopulations rise only modestly and stay at low, stable levels.

Table 3. Results of numerical simulation by RK4 method for (β = 0.45)

Time (t) year	Sub Population				
	S	E	I	T	R
0	121663	0	792	124	225646
5	121831	31	788	105	227567
10	122027	31	811	108	229452
15	122249	32	833	111	231325
20	122499	33	853	113	233185
25	122776	33	870	116	235035
30	123079	34	886	118	236872
35	123410	34	899	120	238698
40	123767	35	911	121	240513
45	124151	35	921	123	242317
50	124561	35	929	124	244109
55	124997	35	935	125	245891
60	125459	35	940	125	247662
65	125947	35	943	126	249423
70	126459	35	944	126	251175
75	126995	35	945	126	252917
80	127556	35	944	126	254650
85	128140	35	943	126	256375
90	128746	35	940	126	258093
95	129375	35	936	125	259803
100	130024	35	932	125	261507

For the higher values $(\beta = 0.45, 0.70)$, especially $\beta = 0.70$, Infected and Treatment subpopulations rise sharply before settling at a much higher plateau, while Susceptible individuals show the deepest decline. The Recovered subpopulation (Figure 6) increases steadily for all four values, growing fastest and largest under the highest transmission rate.

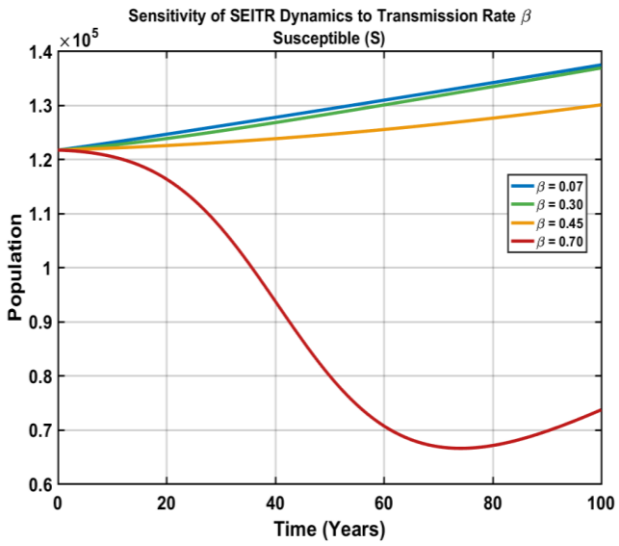

Figure 2. Susceptible (S) for four values of β

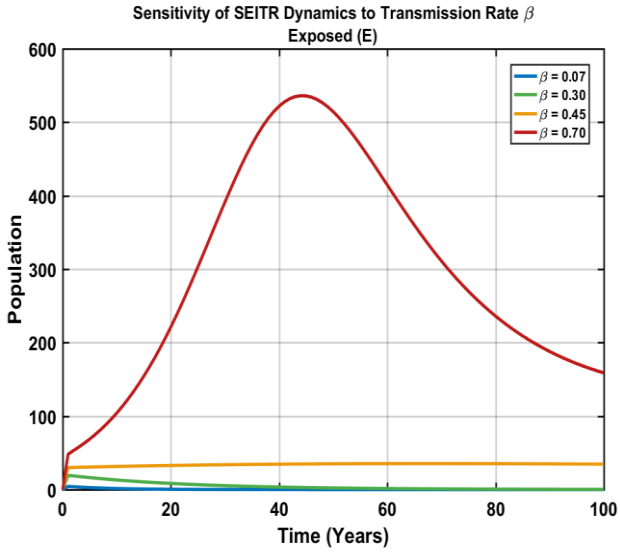

Figure 3. Exposed (E) for four values of β

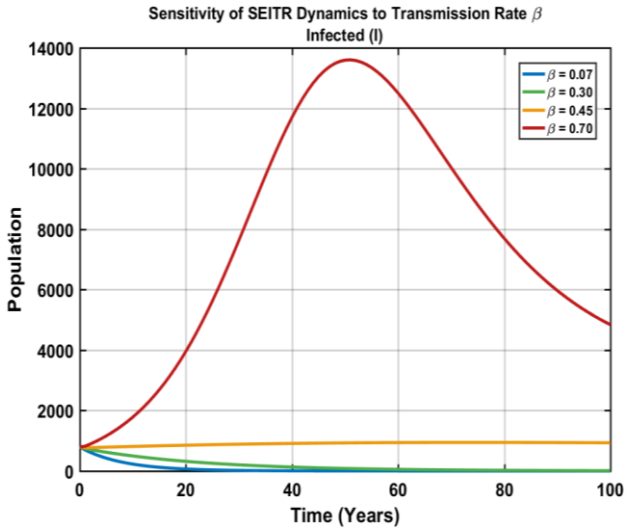

Figure 4. Infected (I) for four values of β

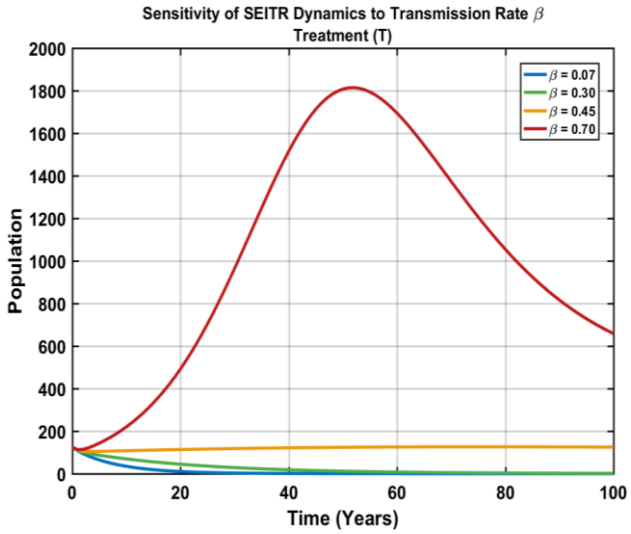

Figure 5. Treatment (T) for four values of β

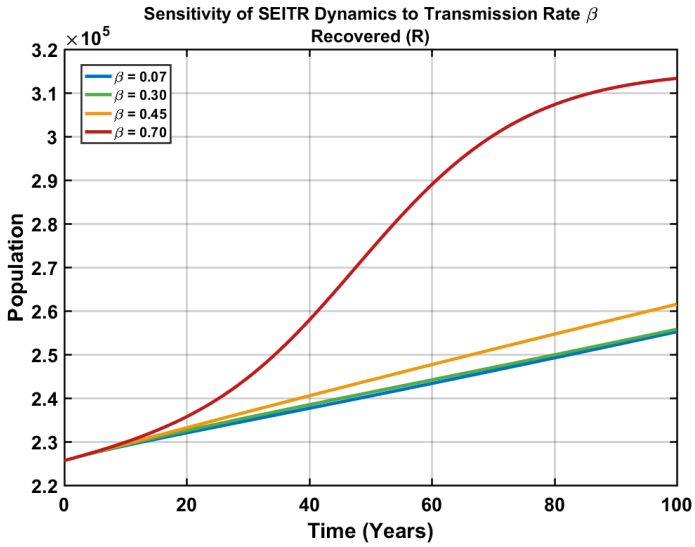

Figure 6. Recovered (R) for four values of β

Figure 7 displays the Infected subpopulation at $t = 150$ years, obtained from 40 simulations with β uniformly sampled from $[0.01, 1]$. For small transmission rates $(\beta < 0.3)$, the infection is effectively absent. The curve then undergoes a rapid, almost vertical ascent over a short β interval, after which the growth moderates considerably. This pattern illustrates a stark dichotomy in long term behavior: meager transmission leads to disease fade out, while robust transmission fosters persistent endemic maintenance

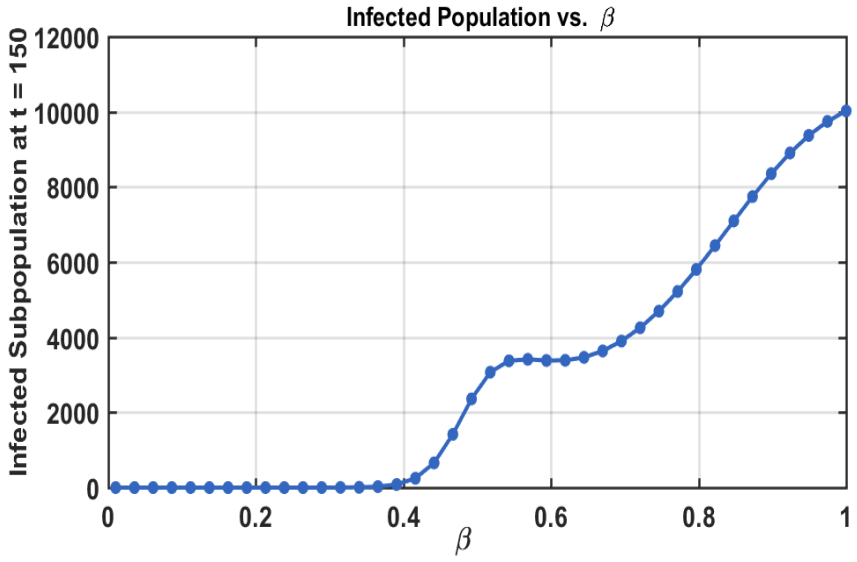

Figure 7. Infected subpopulation vs. β at $t = 150$

6. Comparison Between the RK4 and MATLAB ode45

As an independent check, the same system was solved using MATLAB's adaptive solver ode45 [15] ($RelTol = 10^{-10}, AbsTol = 10^{-12}$) for $\beta = 0.45$ over the full 100 years. Since ode45 shares no algorithmic structure with the fixed step RK4 implementation, agreement between the two solutions provides evidence that the governing equations were correctly translated into code, independent of the specific integration method.

Table 4 compares the final state values ($t = 100$): absolute differences range from 1.53×10^{-11} *to* 1.46×10^{-9} across all five subpopulations, several orders of magnitude below any epidemiologically meaningful quantity. Figure 8 confirms this agreement is sustained throughout the simulation, with differences remaining approximately within $10^{-14} - 10^{-8}$ at every simulated year; the largest deviations (up to 5×10^{-8}) occur within the first three years, coinciding with the fast transient dynamics driven by $\alpha = 4$.

Table 4. Comparison between the RK4 and MATLAB ode45 for (t= 100 years, β = 0.45)

Subpopulation	RK4	ode45 (MATLAB)	Absolute Difference
S	130024.2388994109	130024.2388994106	3.201421×10^{-10}
E	34.6239699878	34.6239699883	5.008118×10^{-10}
I	932.3536701766	932.3536701761	5.195488×10^{-10}
T	124.5995351792	124.5995351792	1.534772×10^{-11}
R	261506.7750664740	261506.7750664741	1.455192×10^{-9}

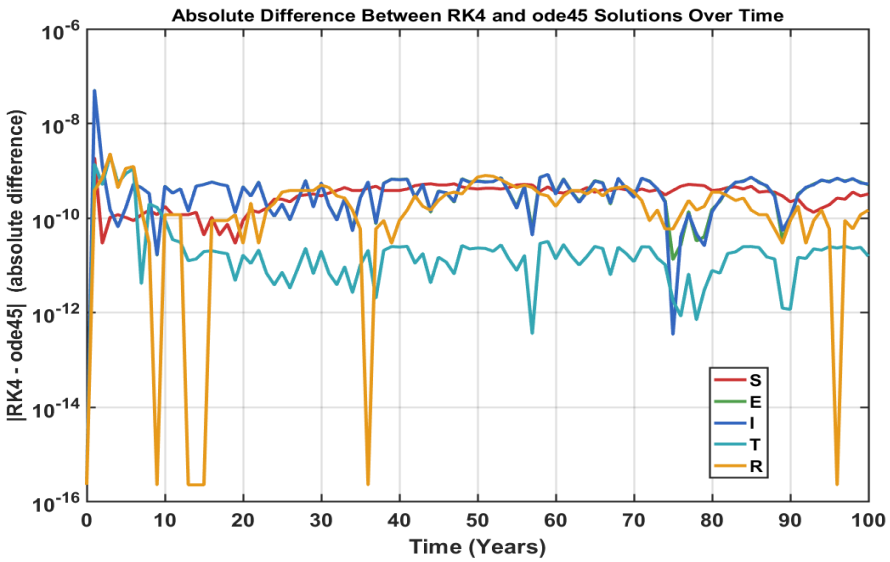

Figure 8. Absolute difference between the RK4 and ode45 solutions for all five subpopulations

7. Order of Convergence Test for the RK4 Method

The classical RK4 scheme has a global error satisfying $\text{Error}(h) \approx C \cdot h^4 \, as \, h \to 0$ [17], where $\text{Error}(h)$ is the L2-norm difference between the numerical solution at step size h and a high accuracy reference solution ($\text{h\_ref} = 2 \times 10^{-4}$). Halving h should therefore reduce the error by a factor near $2^4 = 16$, i.e., $log_2[\text{Error}(h)/\text{Error}(h/2)] \approx 4$ a standard diagnostic for verifying the achieved order of accuracy independently of any analytical error bound. The test was applied to $\beta = 0.45$ over a two year, chosen because the Exposed and Infected subpopulations exhibit their fastest transient dynamics during this period ($\alpha = 4$), making discretization error largest and easiest to detect. Six successive step size halving were tested; results are summarized in Table 5 and Figure 9.

For every halving, the computed $log_2(\text{Ratio})$ remained close to 4, ranging from 4.09 to 4.53 across the tested range down to $h = 0.00625$, with the global error decreasing along a straight line on the $log - log$ scale that closely tracks the theoretical slope of 4. This confirms that the implemented RK4 method achieves its theoretically expected fourth order accuracy

Table 5. RK4 order of convergence results for ($t = 2 \, years, \beta = 0.45$)

h (years)	Global Error (L2 norm)	Ratio Error(h)/Error($h/2$)	log_2(Ratio)
0.20000	7.152075×10^{-4}	—	—
0.10000	3.102007×10^{-5}	23.06	4.53
0.05000	1.643453×10^{-6}	18.87	4.24
0.02500	9.475073×10^{-8}	17.35	4.12
0.01250	5.711642×10^{-9}	16.59	4.05
0.00625	3.361746×10^{-10}	16.99	4.09

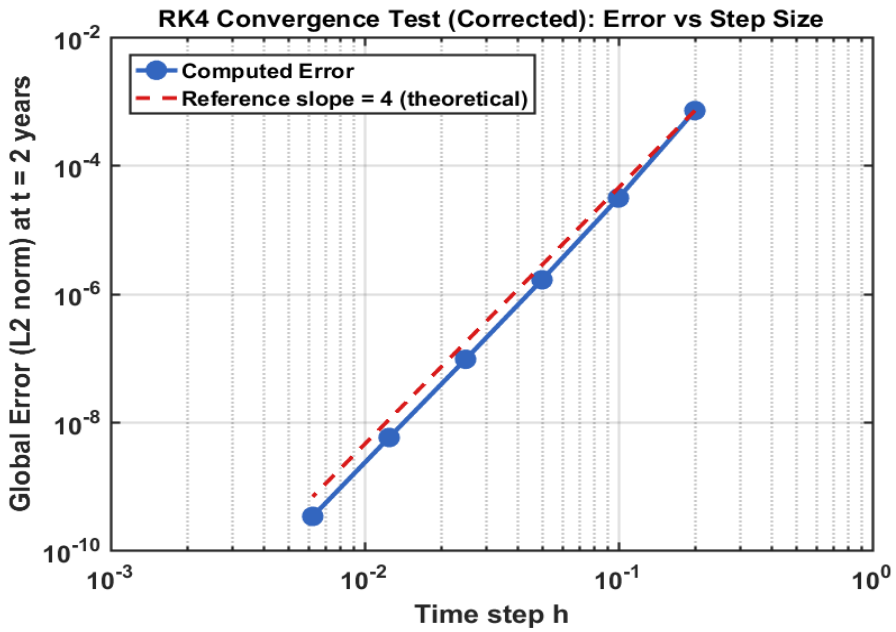

Figure 9. Compared global error with the theoretical four order reference slope

8. Conclusion

This study formulated a SEITR model with standard incidence ($\beta SI/N$) for hepatitis B transmission and solved it using the fourth order Runge Kutta method. The model was parameterized using real demographic data from Ambon, Indonesia. The correctness of the numerical solution was established through three independent procedures. An order of convergence test confirmed that the global error decays at the theoretical fourth order rate. Cross validation against MATLAB's ode45 solver reproduced the same trajectories with absolute differences never exceeding 10^{-8} throughout the 100-year simulation, and as low as $10^{-11} - 10^{-9}$ at the final state, confirming the correctness of the coded equations. A sensitivity analysis across a range of β values showed that the Infected subpopulation increases with transmission intensity, consistent with the expected epidemiological behavior of the model**.** Together, these results confirm that the numerical implementation is accurate and reliable, and establish a rigorous framework for verification. Future work may extend this framework to fractional-order derivatives, time-varying vaccination strategies, or stochastic formulations, using the same verification approach.

References

[1] A.R. McLean, B.S. Blumberg, “Modelling the impact of mass vaccination against hepatitis B. I. Model formulation and parameter estimation,” Proc. R. Soc. Lond. B, Vol. 256(1345), 7-15, 1994.

[2] P. Liang, J. Zu, G. Zhuang, “A Literature review of mathematical models of hepatitis B virus transmission applied to immunization strategies from 1994 to 2015,” J. Epidemiol., Vol. 28(5), 221-229, 2018.

[3] B.O. Emerenini, S.C. Inyama, “Mathematical model and analysis of transmission dynamics of Hepatitis B Virus,” arXiv:1710.11563, 2018.

[4] T. Xue, L. Zhang, X. Fan, "Dynamic modeling and analysis of Hepatitis B epidemic with general incidence," Mathematical Biosciences and Engineering, Vol. 20(6), 10883-10908, 2023.

[5] H.W. Hethcote, "The mathematics of infectious diseases," SIAM Review, Vol. 42(4), 599-653, 2000.

[6] C. Vargas-De-León, "On the global stability of SIS, SIR and SIRS epidemic models with standard incidence," Chaos, Solitons & Fractals, Vol. 44(12), 1106-1110, 2011.

[7] O.M. Otunuga, M.O. Ogunsolu, "Qualitative analysis of a stochastic SEITR epidemic model with multiple stages of infection and treatment," Infectious Disease Modelling, Vol. 5, 61-90, 2019.

[8] S.E. Larubun, Z.A. Leleury, Y.A. Lesnussa, S.P. Tahalea, M.M. Warong, "Dynamic analysis of SEITR mathematical model on the spread of Hepatitis B Disease in Ambon City," Barekeng: Journal of Mathematics and Its Applications, Vol. 18(3), 1989-2000, 2024.

[9] A. Papalia, Y.A. Lesnussa, M.E. Rijoly, O.J. Peter, "Numerical solution of the SEIR model using the fourth-order Runge-Kutta method to predict the spread of Hepatitis B disease in Ambon City," Barekeng: Journal of Mathematics and Its Applications, Vol. 18(3), 2047-2056, 2024.

[10] R.U. Hurit, S. Mungkasi, "The Euler, Heun, and fourth order Runge-Kutta solutions to SEIR model for the spread of meningitis disease," Mathline: Jurnal Matematika dan Pendidikan Matematika, Vol. 6(2), 140-153, 2021.

[11] R. Ashgi, M.A.A. Pratama, S. Purwani, "Comparison of numerical simulation of epidemiological model between Euler method with 4th Order Runge Kutta method," International Journal of Global Operations Research, Vol. 2(1), 37-44, 2021.

[12] A.A. Khoiri, O.P. Perdana, S. Purwani, "Analysis of numerical stability and step size bounds of the fourth-order Runge-Kutta in solving the SEIR epidemiological model," World Scientific News, Vol. 217, 96-107, 2026.

[13] A. Essam, A.R. Hadhoud, T. Radwan, A.A.M. Rageh, I.M. Hanafy, A.M. Abd-Elal, "Numerical simulation of transmission dynamics of the HBV model of fractional-order via a generalized Runge–Kutta Method," Fractal and Fractional, Vol. 10(3), 145, 2026.

[14] H. Abboubakar, S.A.G. Banbeto, R. Jan, R. Fandio, H.P.E. Fouda, I. Khan, M.S. Khan, "Fractional order modeling of hepatitis B virus transmission with imperfect vaccine efficacy," Scientific Reports, Vol. 15, 14245, 2025.

[15] A.A.H. Mtawal, A.A.F. Ali, M.A.H. Haider, "Hybrid technique for solving the fractional-order SIR epidemic model," WSEAS Transactions on Biology and Biomedicine, Vol. 23, 137-146, 2026.

[16] L.F. Shampine, M.W. Reichelt, "The MATLAB ODE Suite," SIAM Journal on Scientific Computing, Vol. 18(1), 1-33, 1997.

[17] R.L. Burden, J.D. Faires, A.M. Burden, "Numerical Analysis, 10th ed.," Boston, MA: Cengage Learning, 2015.